

# Supplementary Information: Wide gap Chern Mott insulating phases achieved by design

Hongli Guo<sup>1,2</sup>, Shruba Gangopadhyay<sup>3</sup>, Rossitza Pentcheva<sup>4</sup>, and Warren E. Pickett<sup>3,\*</sup>

<sup>1</sup>*ICQD/Hefei National Laboratory for Physical Sciences at Microscale,  
and Key Laboratory of Strongly-Coupled Quantum Matter Physics,*

*Chinese Academy of Sciences, and Department of Physics,  
University of Science and Technology of China, Hefei, Anhui 230026, China*

<sup>2</sup>*Synergetic Innovation Center of Quantum Information & Quantum Physics,  
University of Science and Technology of China, Hefei, Anhui 230026, China  
Duisburg-Essen and*

<sup>3</sup>*Department of Physics, University of California Davis,  
One Shields Avenue, Davis, California 95616, USA\**

(Dated: July 27, 2016)

Here we provide additional information on our study of the  $(\text{LaXO}_3)_2/(\text{LaAlO}_3)_4$  (111) superlattices,  $X = \text{Os}$  and  $\text{Ru}$ . The  $X^{3+}$  ion has a  $5d^5$  configuration, and the octahedral coordination splits the  $e_g$  states well above  $t_{2g}$ . The trigonal crystalline field arising from the (111) growth will split the threefold  $t_{2g}$  into  $e'_g + a_{1g}$ , and the symmetric expression adapted to trigonal symmetry for  $t_{2g}$  orbitals is

$$|\Psi_m\rangle = i \frac{1}{\sqrt{3}} (\zeta_m^0 |d_{xy}\rangle + \zeta_m^0 |d_{yz}\rangle + \zeta_m^2 |d_{xz}\rangle) \quad (1)$$

where  $\zeta_m = e^{2\pi im/3}$ .  $m = \pm 1$  represent the  $e'_g$  orbitals,  $m = 0$  is the  $a_{1g}$  orbital. Also  $m$  is the orbital magnetic quantum number. For the  $t_{2g}$  subshell the dominating feature is a competition between local pseudo-cubic symmetry and the underlying threefold and inversion symmetry (P321) of the ideal layer. Relaxation to  $P1$  symmetry mixes the  $\Psi_m$  orbitals, and will mix in some  $e_g$  character in an amount depending on the crystal field splitting.

Considering  $2 X$  atoms, 3 orbitals and 2 spins, 12  $t_{2g}$  bands are involved. Due to the  $d^5$  configuration, two  $t_{2g}$  bands (“one per metal ion”) will be unoccupied. When time reversal symmetry is broken, and the repulsive interaction  $U$  and the SOC are both included, a topologically Chern insulating phase may be realized.

**Osmate.** The SOC effect on the  $d$ -projected density of states (pDOS) of both Os1 and Os2 sites in 2LOsO is shown in Fig. 1. The upper four panels are for  $a_{LAO}$ , the bilayer that is a Chern insulator with  $C = +2$ . There are very few differences between the pDOS of Os1 and Os2, consistent with the minor distortion during the relaxation from P321 to  $P1$  as mentioned in the main text. Without SOC, a narrow peak overlaps Fermi level, which corresponds to a flat band region. In the trigonal coordinate system, the  $d_{z^2}$  orbital is  $a_{1g}$  character, the rest can be considered to be  $e'_g$  character. The narrow peak is mixed  $a_{1g}$  and  $e'_g$  character. SOC splits this peak,

opening a 46 meV gap corresponding to the band anticrossing occurring near the Fermi level, see Fig. 4 in the main text. As a consequence of this entanglement by anticrossing, a Chern insulating phase is obtained.

The lower four panels are the analogous plots for  $a_{LNO}$ . Here the pDOS of Os1 is much different than that of Os2, which is attributed to the large distortion and symmetry reduction resulting from the strain. The dominant character, the pDOS weight, and the band width of the valence bands are different for the two Os sites. Compared to those for  $a_{LAO}$ , there are no flat band regions, and the gap is already opened before SOC is applied. SOC slightly reduces the gap, and the effect of all the differences is to leave a trivial insulating phase.

**Ruthenate.** Fig. 2 shows the analogous  $d$  pDOS of Ru sites in the 2LRuO bilayer. The upper four panels are for  $a_{LAO}$ , which is a trivial insulator; the lower four are for  $a_{LNO}$ , which is Chern insulator with  $C=-1$ . Again for the Chern insulating phase, the Ru1 and Ru2 sites are almost equivalent in their electronic structure. For trivial insulating phase, however, the Ru1 and Ru2 sites have differing  $d$  electronic structures. The narrow peak which reflects the flat band region near the Fermi level exists for both lattice constants; that of  $\text{Ru}@a_{LAO}$  is dominated by  $d_{xy}$  electrons, while that of  $\text{Ru}@a_{LNO}$  also has  $a_{1g}$  character – the same situation as for the Chern insulating 2LOsO bilayer. Notably, for  $\text{Ru}@a_{LNO}$ , the narrow peak before SOC splits and opens a 132 meV gap, which combined with band anticrossing produces the Chern insulating phase. Both Chern insulating bilayers have holes primarily of  $a_{1g}$  character.

**Energy-resolved Chern number.** The energy-resolved (*i.e.* variable chemical potential) Chern number is provided in Fig. 3. It is apparent that the coefficient of  $e^2/h$  accurately attains the integer  $C = 2$  value for 2LOsO across the 46 meV gap, and attains  $C=-1$  for 2LRuO over its 132 meV gap.

---

\* pickett@physics.ucdavis.edu

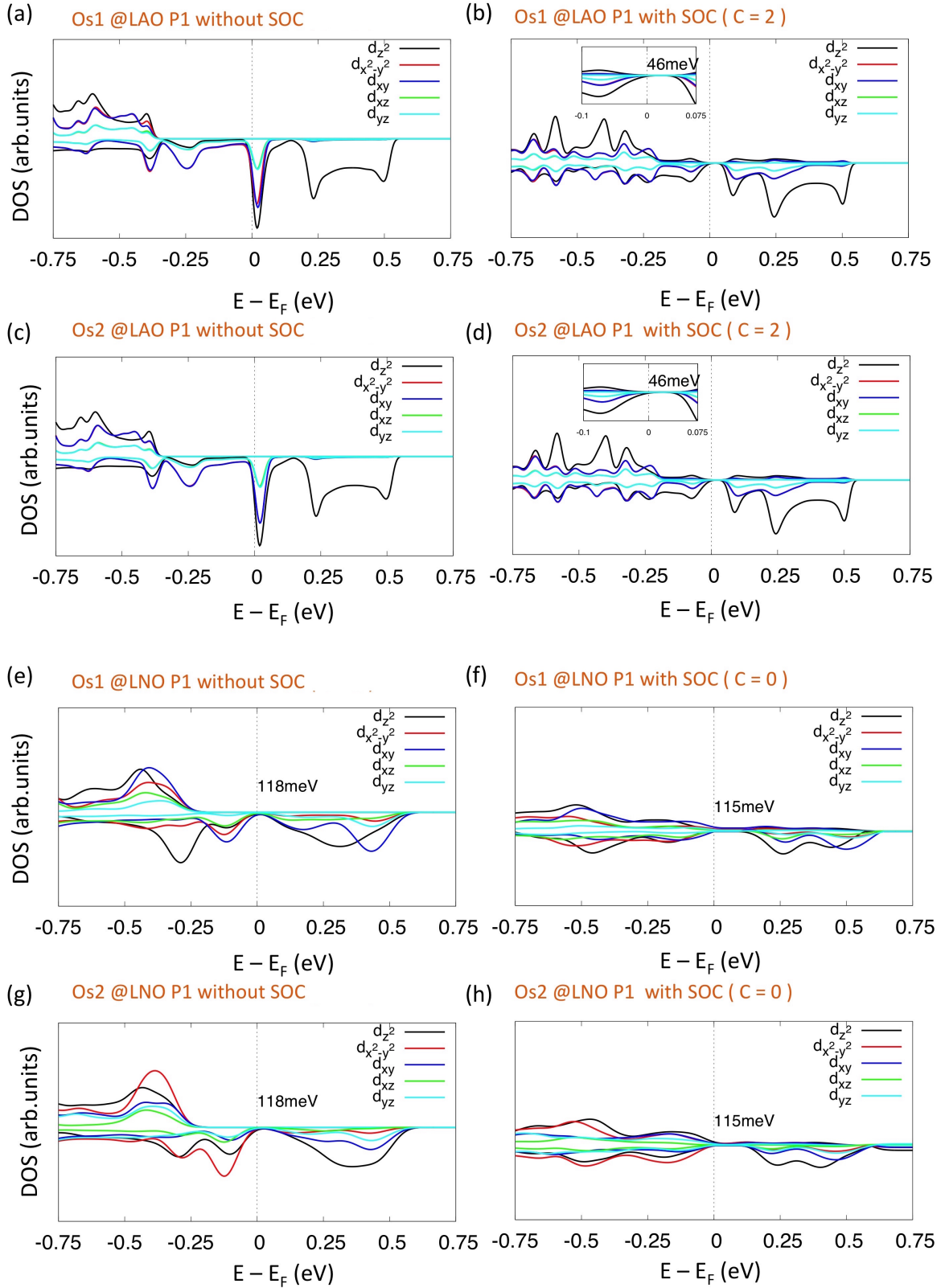


FIG. 1. The  $d$  projected density of states of the two inequivalent Os atoms in 2LOsO bilayers with P1 symmetry. The left panels, before including SOC; right panels, with SOC included. Upper four panels (a,b,c,d): pDOS of the two Os in 2LOsO bilayers corresponding to lattice constant  $a_{LAO}$ ; lower four panels (e,f,g,h): analogous plots for  $a_{LNO}$ .

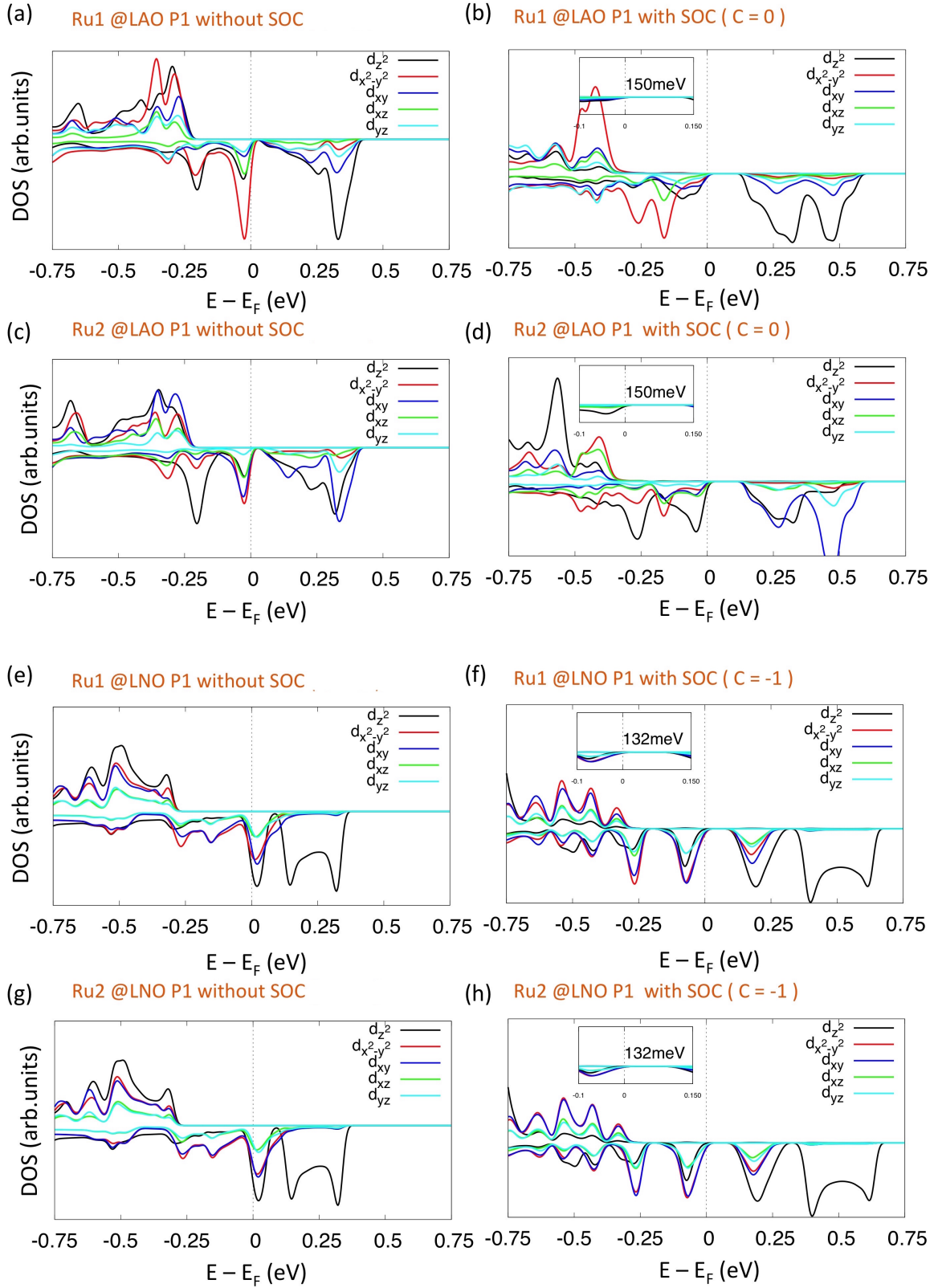


FIG. 2. As for Fig. 1, but for 2LRuO.

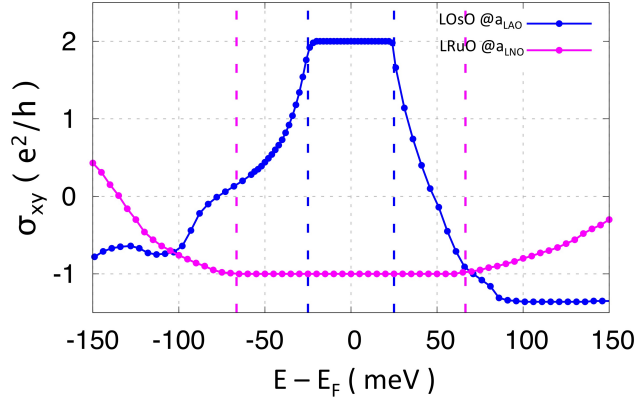


FIG. 3. The calculated anomalous Hall conductivity  $\sigma_{xy}$ , plotted in units of  $e^2/h$  versus the chemical potential. Curves for both of the Chern insulator states are shown. The flat region indicates the gap, whose edges are given by dashed vertical lines. The relative positioning of the two curves is irrelevant.